Research Square

Preprints are preliminary reports that have not undergone peer review.
They should not be considered conclusive, used to inform clinical practice,
or referenced by the media as validated information.

Wildfire susceptibility and response accessibility mapping for forest fire management in Mizoram, India

Madhuparna Majumder
Energy and Resources Institute
Sayanta Ghosh
sayanta.ghosh@teri.res.in
Energy and Resources Institute
Jitendra Vir Sharma
Energy and Resources Institute

Research Article

Keywords: Wildfire susceptibility, Analytical Hierarchical Process (AHP), Geographical Information System (GIS), network analysis, service-area mapping, response accessibility, resource allocation, Mizoram, Northeast India

Posted Date: June 5th, 2026

DOI: https://doi.org/10.21203/rs.3.rs-9702636/v1

License: This work is licensed under a Creative Commons Attribution 4.0 International License.
Read Full License

Additional Declarations: No competing interests reported.

Wildfire susceptibility and response accessibility mapping for forest fire management in Mizoram, India

Madhuparna Majumder[1], Sayanta Ghosh[1*] and Jitendra Vir Sharma[1]
[1]*The Energy and Resources Institute, New Delhi*
(*Corresponding author: sayanta.ghosh@teri.res.in ***)***

Abstract

Mizoram in northeast India faces recurring forest fires in a climatically fragile, steep and densely forested landscape. This amplifies risks to forest resources, biodiversity, air quality and forest-dependent communities including indigenous peoples. This study integrates AHP and GIS-based network analysis to develop an operational framework for wildfire vulnerability zoning and response resource planning. A multi-source geospatial database was prepared using historical fire occurrences and key drivers covering vegetation and land use, topography, bio-climatic variables, and human influence indicators. Using AHP, criteria were weighted through pairwise comparisons with acceptable consistency and combined to delineate wildfire susceptibility into four classes, low, moderate, high, and extremely high. The susceptibility map indicates that about 0.5% of the state falls under very high susceptibility, about 58% under high, and about 36% under moderate susceptibility, implying that over 90% of the landscape warrants targeted prevention and preparedness planning. To translate risk zoning into response readiness, service-area and proximity analyses were conducted using the road network and existing fire response locations under time thresholds relevant for initial attack. Current coverage is limited, with only about 9% of the area reachable within 15 minutes and about 11% within 30 minutes, indicating substantial response gaps in high-risk zones. The integrated outputs identify priority landscapes where prevention infrastructure, strategic placement of suppression teams and connectivity improvements can most effectively reduce response time and impacts. The approach supports context-specific operational planning and evidence-based policy decisions and is transferable to other mountainous fire-prone regions where accessibility strongly shapes fire outcomes.

Keywords: Wildfire susceptibility, Analytical Hierarchical Process (AHP), Geographical Information System (GIS), network analysis, service-area mapping, response accessibility, resource allocation, Mizoram, Northeast India

1. Introduction

Forests are among the most important terrestrial carbon reservoirs, storing nearly 39% of global terrestrial carbon (Lu, 2025). By absorbing atmospheric CO_2 through photosynthesis

and retaining carbon in above-ground and below-ground biomass and soils, they play a central role in climate regulation and the global carbon cycle (Brown, 1997). Tropical forests, in particular, strongly influence global carbon fluxes through the balance of carbon uptake and release (Mitchard, 2018). However, this balance is increasingly being disrupted as forest fire regimes intensify under a warming climate, with rising fire activity and shifts in vegetation dynamics (Williams et al., 2023; Zhang et al., 2024). Recent years have witnessed a marked escalation in wildfire impacts worldwide; 2024 was reported as the most extreme year for forest fires on record, with at least 13.5 million hectares of forest burned, exceeding the previous record set in 2023 by about 13% (MacCarthy et al., 2025). Such increases in burned area drive higher emissions of CO_2 and other greenhouse gases, often outpacing the capacity of forests to re-sequester carbon (Walker et al., 2025; Jiang et al., 2023; Zhao et al., 2021), and raising the risk of landscapes shifting from net carbon sinks to net carbon sources (Eckdahl et al., 2022). Beyond carbon impacts, wildfire smoke poses major public health risks through acute and chronic exposure to fine particulate matter $PM_{2.5}$ (Reid et al., 2016), while also undermining the livelihoods of forest-dependent communities (Revich, 2024).

India, with forests covering 21.67% of its land area (Kumar, 2024), has experienced a worrying rise in wildfire frequency and intensity over recent decades (Sewak et al., 2021). Nearly 36% of India's forests are considered susceptible to recurrent fires, with Northeast India, Uttarakhand, Madhya Pradesh, and Chhattisgarh reporting frequent fire incidents in recent years (Goparaju et al., 2023). Evidence from multiple studies indicates that more than 90% of fire occurrences originate from human actions, with meteorological conditions such as elevated temperature, low humidity, and strong winds frequently intensifying fire behaviour and spread (Bera et al., 2022, Chaudhary et al., 2022, Khan et al., 2024; Gupta et al., 2023). Forest fires also disrupt local livelihoods by limiting access to non-timber forest products that often serve as critical income sources (Saxena et al., 2022). These interacting pressures underscore the need for proactive management strategies that can strengthen forest resilience under a changing climate (Reid et al., 2016).

In this context, GIS and remote sensing have become essential for forest fire risk assessment and prioritisation (Novković et al., 2021). They enable the integration of spatial information on topography, vegetation, climate, and anthropogenic pressures to identify areas most vulnerable to ignition and spread, and to generate spatially explicit risk maps that support targeted mitigation and efficient resource allocation (Hai et al., 2023). For such multi-dimensional risk settings, the AHP is a widely applied Multi-Criteria Decision-Making (MCDM) approach that supports transparent weighting and prioritisation of risk factors and has proven particularly effective when integrated with GIS for spatial fire-risk assessments (Rahmati et al., 2015). This is especially relevant for vulnerable settings where environmental hazards interact with economic and social constraints (Kumar et al., 2025).

The present research focuses on Mizoram, located in the north-eastern region of India. According to the India State of Forest Report 2017, Mizoram ranked first in deforestation,

losing 531 km² over two years, with forest fires identified as a major contributing factor (FSI, 2017). Mizoram also records the highest number of fire incidents in the country, accounting for roughly one-third of the forest fire instances in the northeast region (Tripathi et al., 2020). Low moisture conditions in forested landscapes further contribute to fire occurrence and spread, reinforcing the need for systematic fire-risk evaluation to support sustainable forest management and disaster prevention (Olaniya et al., 2020). Despite these concerns, the study area lacks a comprehensive and cohesive modelling framework for delineating forest fire risk zones. This study addresses that gap by developing a systematic geospatial framework to support the design and implementation of effective prevention and mitigation measures for forest fires in Mizoram.

2. Study Area

Mizoram lies in northeast India between 92°16′E and 93°26′E longitude and 21°56′N and 24°31′N latitude (Figure 1). The state covers about 21,081 square kilometres, of which nearly 85% is under forest cover, amounting to approximately 17,990 square kilometres (ISFR, 2023). Mizoram receives high rainfall, with annual precipitation typically ranging from 2500 mm to 3000 mm (Mizoram State Climate Change Cell, 2023). The terrain is predominantly steep and rugged, with elevations ranging from about 50 m to over 2000 m above mean sea level. Vegetation in Mizoram varies with altitude and rainfall and is broadly classified as Tropical Wet Evergreen Forest, Montane Sub-Tropical Forest, and Temperate Forest (ISFR, 2023). The climate is generally mild, with winter temperatures typically between 11 and 21 °C and summer temperatures between 20 and 30 °C. The India State of Forest Report 2023 further indicates that around half of the forests in Mizoram are highly susceptible to wildfires. As per the Champion and Seth Forest classification, the dominant forest types include Secondary moist bamboo brakes at 36.37%, East Himalayan moist mixed deciduous forest at 32.21%, and Cachar semi-evergreen forest at 30.44% based on the Forest Cover Map from ISFR 2023.

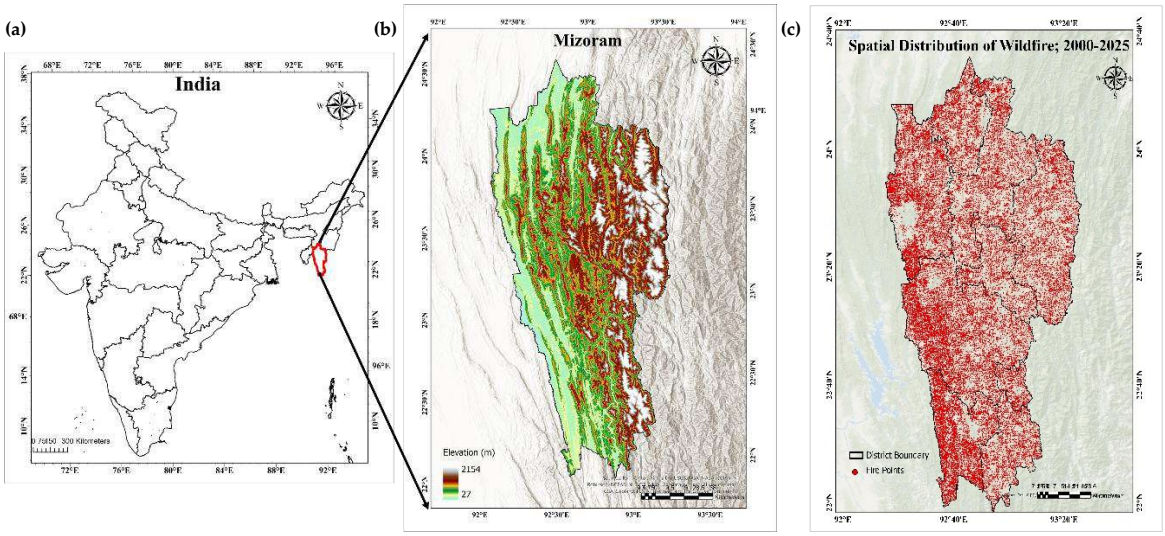


Figure 1 (a) Mizoram's geographical location; (b) Elevation; and (c) Spatial distribution of wildfires in (2000-2025)

3. Dataset & Methodology

The methodology involved the following steps: developing a comprehensive database for wildfire vulnerability assessment by collecting samples of historical wildfires and related indicators, identifying vulnerable parameters that act as drivers of wildfires and integrating them with the AHP model to assess the impact of classification criteria and weighting methods on vulnerability modelling, and conducting proximity analysis to guide strategic resource allocation based on the vulnerability results. The overall methodology is shown in below Figure 2.

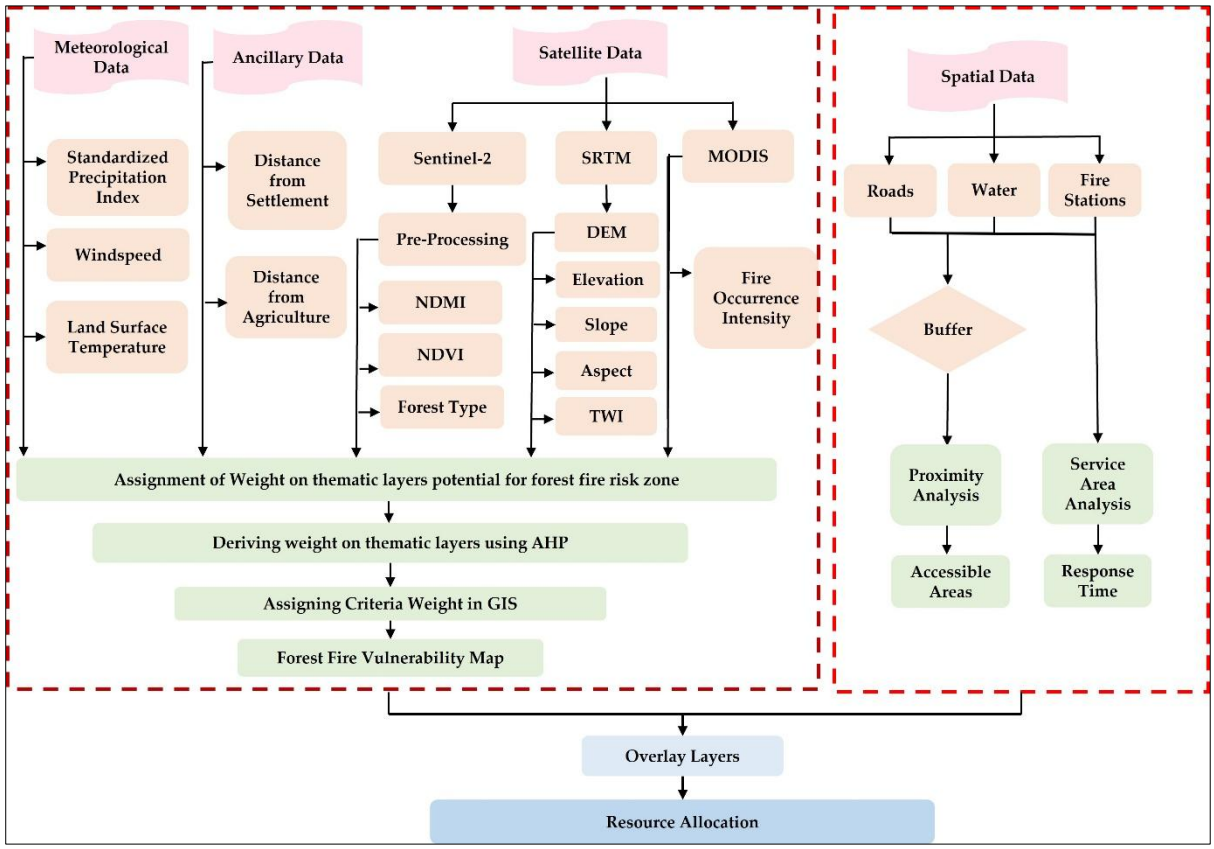


Figure 2 Overall Methodological Framework

3.1. Thematic Layer Preparation

The selection of thematic layers was based on their relevance in both natural and man-made factors that contribute to the incidence and spread of wildfires. These factors were divided into five categories: topographic, climatic, vegetation, forest cover and anthropogenic. Topographic factors, such as Elevation and Aspect, influence the local microclimate conditions. The Topographic Wetness Index (TWI) is used to describe the accessibility of water sources and surface wetness (Pourtaghi et al., 2015; Zhang et al., 2021), while Slope and curvature affect fire spread patterns (Ghorbanzadeh et al., 2019; Yang et al., 2021; Nikolić et al., 2023). Vegetation characteristics, such as forest type represent the available fuel load and potential combustion capacity (Rihan et al., 2019; Bergonse et al., 2021). Land Surface Temperature (LST), Standardized Precipitation Index (SPI), and Windspeed were included as

important meteorological and climatic indicators; LST reflects surface heat conditions, suggesting vegetation and soil dryness; higher LST values are associated with reduced fuel moisture and increased vulnerability to fire ignition and rapid spread. SPI measures precipitation anomalies in relation to long-term climatology, with negative values indicating drought-affected areas with more combustible vegetation. Wind speed controls the rate and direction of fire propagation by influencing flame tilt, convective heat transfer, and ember transport. Anthropogenic factors reflect human activity and infrastructure proximity, including distance to agriculture and settlement (Elia et al., 2020; Wu et al., 2023). A summary of these factors, including their sources, is provided in Table 1.

Table 1 Data Sources

Factors	Parameters	Data Source
Topographic Factors	Slope	SRTM DEM (30m)
	Aspect	SRTM DEM (30m)
	Elevation	SRTM DEM (30m)
	Topographic Wetness Index (TWI)	SRTM DEM (30m)
Climatic Factors	Land Surface Temperature (LST)	MODIS / Terra
	Standardized Precipitation Index (SPI)	TerraClimate (4km)
	Wind Speed	TerraClimate (4km)
Vegetation &Moisture Indices	Normalized Difference Vegetation Index (NDVI)	Sentinel-2 (10m)
	Normalized Difference Moisture Index (NDMI)	Sentinel-2 (10m)
Forest Cover & Fire Occurrence Areas	Forest Type	Sentinel-2 (10m)
	Fire Occurrence Intensity	MODIS VIIRS
Anthropogenic Factors	Distance to Settlements and Agriculture	GHSL, GFSAD

1. Forest Type/Vegetation Type: (FT):

The fuel properties of various vegetation varieties are distinct, which is why vegetation characteristics are critical determinants of fire susceptibility (Pyne, 1997). Areas with dense vegetation and low moisture content are more susceptible to ignition, while vegetation with higher moisture and lower density is more resistant to fire. During protracted periods of mild and dry weather, the accumulation of dry fuel further increases the likelihood of fire initiation and sustains propagation (Taylor et al., 2006). In natural ecosystems, such as grasslands or bush/scrub areas, uncontrolled combustion is highly contingent upon the availability of fuel and the current environmental conditions (Gill, 1975). The International Geosphere-Biosphere Program (IGBP) vegetation layer was obtained from the MODIS Land Cover Type product, which generates annual global land cover maps according to the 17-class IGBP classification scheme. The consistent, globally standardized vegetation classification of the NASA MODIS Land Cover Type Collection (MCD12Q1/MCD12C1) was employed from Terra and Aqua data. NDVI values were extracted for the same period, and pixel-wise statistics were

calculated for each IGBP class. The NDVI raster was subsequently reclassified to align with IGBP categories based on observed spectral patterns and cross-validated with the original layer. This resulted in a harmonized vegetation map that maintained IGBP interpretability while incorporating region-specific variability for fire vulnerability assessment.

2. Normalized Difference Moisture Index (NDMI):

NDMI is employed to evaluate the moisture content of vegetation, which has a direct impact on the susceptibility of an area to wildfires. NDMI is calculated from near-infrared (NIR) and shortwave-infrared (SWIR) reflectance as: *NDMI = (NIR – SWIR) / (NIR + SWIR).* Moist vegetation is indicated by higher NDMI values, whereas arid, more flammable fuels are indicated by lower NDMI values. MODIS derived NDMI was resampled to match the grid resolution of other factors (Rihan et al., 2019; Bergonse et al., 2021).

3. Fire Occurrence Intensity (FPI):

Fire occurrence intensity is a standardized derived layer, can be developed using Fire Radiative Power (FRP) extracted from historical fire datasets spanning 2000-2025, such as MODIS and VIIRS active fire products, which provide daily observations of wildfire locations. FRP being a physically based indicator of radiative energy release, provides a proxy for fire intensity and combustion dynamics. Historical MODIS/VIIRS fire records allow mapping of spatiotemporal fire patterns, identifying fire-prone areas, peak fire seasons, and repeat burn locations, which are crucial for validating fire vulnerability models (Li et al., 2018). To generate continuous spatial fire intensity surfaces, Inverse Distance Weighting (IDW) interpolation was applied to the historical fire occurrence points, allowing the creation of gridded maps representing fire frequency and intensity patterns.

4. Normalized Difference Vegetation Index (NDVI):

NDVI is extensively utilized to assess vegetation health, density, and production, factors that affect wildfire vulnerability. NDVI is calculated from red (R) and near-infrared (NIR) reflectance as: NDVI = (NIR – R) / (NIR + R). Higher NDVI values mean that the vegetation is thick and healthy, while lower values mean that the vegetation is sparse or stressed, which may make fires more likely. For this study, NDVI was derived from Sentinel-2 satellite data, resampled to the standard grid resolution, and incorporated into the fire vulnerability model to account for spatial variation in vegetation cover and potential fuel load (Rihan et al., 2019; Bergonse et al., 2021).

5. Aspect (A):

The inclination of slopes significantly affects forest fire susceptibility by influencing microclimatic conditions, fuel moisture, and sun radiation. In Mizoram, the east and west-facing slopes experience greater sun exposure, resulting in drier soils and flora, hence enhancing flammability and the possibility for fire spread. In contrast, north- and northeast-

facing slopes often maintain greater moisture levels and sustain denser, less fire-susceptible vegetation (NESAC, 2014). Incorporating aspect into fire vulnerability assessments helps identify areas where slope orientation may exacerbate fire risk, enabling more accurate mapping of high-risk zones and targeted allocation of fire management resources in the state's hilly terrain.

6. Slope (S):

The slope angle significantly affects fire behaviour. As the steepness of the slope rises, both fire intensity and pace of spread often escalate (Agee, 1993). Steeper slopes increase the radiant heat exposure to unburned fuel while diminishing convective heat loss, resulting in accelerated preheating and easier ignition of fuels. Slope also affects the fire's interaction with wind: on steep slopes, fires can advance uphill even against prevailing winds due to enhanced upslope draught, whereas on gentler slopes, wind may inhibit uphill spread (Cruz et al., 2003; Riley et al., 2020).

7. Elevation (E):

Elevation affects fire dynamics by influencing precipitation patterns, wind exposure, and the seasonal desiccation of fuels (Agee, 1993; Cruz et al., 2003). At reduced altitudes, elevated temperatures coupled with less precipitation expedite fuel desiccation, heightening fire vulnerability earlier in the season. Elevated regions are also susceptible to lightning strikes, which can act as natural ignition sources for wildfires. (Cruz et al., 2003; Moritz et al., 2014).

8. Standardized Precipitation Index (SPI):

Fire susceptibility is significantly affected by precipitation patterns, which may be measured using the Standardized Precipitation Index (SPI). SPI quantifies the deviation of recorded precipitation from long-term average values, normalizing it to discern dry or wet situations. It is calculated as: $SPI = (P–\bar{P})/\sigma P$, where P is the observed precipitation over a specified period, $\bar{P}$, is the long-term mean precipitation, and σP is the standard deviation of precipitation for that period. Negative SPI values signify dry conditions, characterized by a reduction in soil and vegetation moisture, hence elevating the risk of fire ignition and propagation.

9. Land Surface temperature (LST):

Land Surface Temperature (LST) is a crucial parameter in the Earth's climate system, signifying the transfer of energy and water between the terrestrial surface and the atmosphere. LST also affects plant development and soil moisture, since elevated surface temperatures expedite moisture loss from soils and vegetation, thereby enhancing fuel flammability. This study utilized LST data sourced from the Google Earth Engine platform (MODIS-Terra MOD11C2 v006) at a spatial resolution of 0.05° x 0.05° across a decade (2015–2025).

10. Topographic Wetness Index (TWI):

The Topographic Wetness Index (TWI) is calculated based on the slope and the upslope contributing area per unit width, oriented perpendicular to the flow direction. TWI readings are closely correlated with soil characteristics, such as horizon depth, silt content, organic matter concentration, and phosphorus concentrations (Moore et al., 1993). Elevated TWI values signify regions with more potential for runoff accumulation, whereas diminished values pertain to upslope areas with lesser runoff contribution (Beven & Kirkby, 1979). This study employed the topographic wetness index formula using DEM data to derive it. This model effectively predicts the concentration of water in areas with various altitudes. It is determined by the slope and the area contributing upstream. $TWI = ln\ (a/\tan b)$, Where: a = upslope contributing area (m^2), b = slope in radians.

11. Wind Speed (WS):

Wind speed impacts wildfire propagation by altering flame inclination, convective heat transfer, and the likelihood of spot fires. For this study, data from TerraClimate (4 km resolution, 1958-2025) were used to identify regions susceptible to fast fire spread (Cooke et al., 2012; Bergonse et al., 2021).

12. Distance from Agriculture (DA):

The occurrence of wildfires in Mizoram is significantly influenced by the proximity to agricultural areas, particularly as a result of the practice of jhum cultivation (slash-and-burn farming). The unintentional spread of fires to adjacent forested areas is a common occurrence when crop residues are burned, or fields are cleared for cultivation. The risk of wildfire decreases as the distance from agricultural land increases, as the frequency of ignition sources from human activity decreases and fuel accumulation patterns diverge. (Moritz et al., 2014).

13. Distance from Settlement (DS):

Human activities can exacerbate the incidence of wildfires, especially in regions with significant population and housing movement near villages. Various anthropogenic sources, such as exposed flames, cigarettes, electrical sparks, and vehicles, can function as ignition sources for fires that encounter flammable fuels (Moritz et al., 2014).

To ensure consistency in model development and statistical analyses, all 13 thematic layers were projected onto the UTM Zone 46N coordinate system and resampled to a consistent grid resolution of 10 x 10 m and overlayed to further generate vulnerability map. The coarser resolution climatic parameters such as SPI and LST were not downscaled, or enhanced to a finer resolution, but were resampled solely to achieve spatial consistency with higher-resolution datasets (e.g., Sentinel-based datasets at 10 m) for integrated analysis. The purpose of resampling was to ensure pixel-level alignment and seamless overlay within a unified geospatial framework, without altering the inherent information content of the original data.

3.2. Weight Assignment

In the weight assignment, all input assigned factors were reclassified ranging from 1 to 4, where 1 denotes the least significant (low) and 4 signifies the most significant (very high).

Table 2 Reclassed Value Range of Parameters from low to high based on importance.

Parameters	Class Type	Class	Range	Parameters	Class Type	Class	Range
Forest Type/ Vegetation Type	Grassland, Savannas, Cropland, Woody Savannas	Very high	1	**Standardized Precipitation Index**	-0.18-0	Very High	4
	Evergreen needleleaf, deciduous broadleaf, Mixed Forest	High	2		0-0.25	High	3
	Evergreen Broadleaf	Moderate	3		0.25-0.75	Moderate	2
	Other Classes	Low	4		<1.43	Low	1
NDMI	<0.2	Very high	4	**Land Surface Temperature**	<21	Low	1
	0.2-0.35	High	3		21-22	Mod	2
	0.35-0.5	Moderate	2		22-23	High	3
	>0.5	Low	1		23-26	Very high	4
Fire Occurrence Intensity	0	Low	1	**Topographic Wetness Index**	<8	Very high	4
	0 – 1	Moderate	2		8-12	High	3
	1 – 2	High	3		12-15	Moderate	2
	2 – 3	Very High	4		>15	Low	1
Normalized Difference Vegetation Index	<0.15	Low	1	**Wind Speed**	<1.05	Low	1
	0.15-0.55	Very high	4		1.05-1.15	Moderate	2
	0.55-0.65	High	3		1.15-1.25	High	3
	>0.65	Moderate	2		<1.32	Very high	4
Aspect	E, W	Very high	4	**Distance from Agriculture**	500m	Very High	4
	NE, SE, SW	High	3		500m-1km	High	3
	NW	Moderate	2		1-1.5km	Moderate	2
	N, S, Flat	Low	1		>1.5km	Low	1
Slope	<3	Low	1	**Distance from Settlement**	500m	Very High	4
	3 - 8	Moderate	2		500m-1km	High	3
	8 - 15	High	3		1-1.5km	Moderate	2
	>15	Very high	4		>1.5km	Low	1
	0-500	Moderate	2				

Elevation	500-1000	Very high	4	
	1000-1500	High	3	
	>1500	Low	1	

A pairwise comparison matrix was constructed to assess the relative significance of aspects utilizing the Analytic Hierarchy Process and the Saaty scale, with values spanning from 1 (equal importance) to 9 (extreme importance) shown in Table 3 (Saaty, 1980). The normalized relative weight was determined by dividing each element of the pairwise matrix by the sum of its column. The weights of each layer were determined using the principal eigenvector of the square matrix corresponding to each criterion. The greater the weights, the more significant the influence of the parameters on the forest fire, as determined by their relative relevance.

Table 3 Scale for Pairwise Comparision Matrix

Intensity Importance	Linguistic Variables
1	Equal importance
2	Equal to moderate importance
3	Moderate importance
4	Moderate to the strong importance
5	Strong importance
6	Strong to the very strong importance
7	Very strong importance
8	Very to the extremely strong importance
9	Extreme importance

Weights for each thematic layer were calculated using these equations:

1. Calculate the total of the values in each column of the pairwise comparison matrix utilizing the formula (Eq.1)

$$\boldsymbol{Lij} = \sum_{n=1}^{n} \boldsymbol{Cij} \quad (1)$$

where $\boldsymbol{Lij}$ is the total column value of the pair-wise comparison matrix and $\boldsymbol{Cij}$ is the criteria used for the analysis.

2. Normalize the pair-wise comparison matrix by dividing each member by the sum of its respective row (Eq.2)

$$\boldsymbol{Xij} = \frac{\boldsymbol{Cij}}{\boldsymbol{Lij}} \quad (2)$$

where $\boldsymbol{Xij}$ = normalized pair-wise comparison matrix.

3. Calculate the standard weight by dividing the total of the normalized row of the matrix by the number of criteria/parameters (N) using the following formula (Eq.3)

$$\boldsymbol{Wij} = \frac{\sum_{j=1}^{n} \boldsymbol{Xij}}{\boldsymbol{N}} \quad (3)$$

where Wij = standard weight.

4. The consistency vector values were computed using the following formula (Eq.4)

$$\lambda = \sum_{i=1}^{n} CVij \quad (4)$$

where λ = consistency vector.

5. The following formula was used to calculate the Consistency Index (CI), which is a deviation or degree of consistency (Eq.5)

$$CI = \frac{\lambda - n}{n - 1} \quad (5)$$

where CI = Consistency Index, n = Number of criteria.

6. The formula (Eq.6) is employed to determine the consistency ratio (CR).

$$CR = \frac{CI}{RI} \quad (6)$$

where RI = random inconsistency.

If the Consistency Ratio (CR) is less than or equal to 0.10, the level of inconsistency is deemed acceptable. Random inconsistency (RI) values for 'n' criteria, i.e., parameters.

Table 4 Random Inconsistancy Value (Saaty, 1980)

n	2	3	4	5	6	7	8	9	10	11	12	13	14
RI	0	0.52	0.9	1.12	1.24	1.32	1.41	1.45	1.49	1.51	1.48	1.56	1.57

The overall scores were computed by multiplying the weights of the individual thematic layers by the weights of the features inside each layer, summing the resultant products of all attributes, and applying the formula (Eq.7).

$$TS = \sum W\ X\ R \quad (7)$$

where TS = Total Score, W and R were the weight of the thematic layers and the weight of the features in the thematic layers, respectively.

3.3. Proximity Analysis for Fire Suppression Infrastructure

The resultant vulnerability map was further integrated with GIS-based proximity and network service area evaluations to analyse the accessibility of forested areas for ground firefighting teams within critical response times. For fire suppression infrastructure, proximity analysis evaluates the distribution efficiency of fire stations, water sources, and accessible roadways in fire-prone areas. Euclidean distance or network-based Service Area

analysis is used to construct spatial distance or reaction time buffers around suppression infrastructure to get inside a threshold. Underserved areas may need more infrastructure or road connectivity due to their distance or travel duration. For the analysis, road segments from the OSM dataset were classified into three hierarchical categories: Primary (major highways and arterial routes; facilitate high-capacity and long-distance movement), Secondary (important connector roads; link primary roads to urban centres, towns, and major settlements, and Tertiary(smaller paved roads; provide local-level connectivity within towns and rural areas). The detailed classification of OSM road types used in this study is presented in Table 5.

Table 5 Types of Roads undertaken.

Primary Roads	**Secondary Roads**	**Tertiary Roads**
Primary	Secondary	Tertiary
Primary link	Secondary Link	Tertiary Link
Trunk		Residential
Trunk Link		Service

The investigation omitted unclassified roads, tracks, cycle paths, pedestrian walks, and other minor pathways because fire vehicles cannot use them and may impair operational movement. After cleaning the road network, GIS tools corrected topology problems, removed overlaps and gaps, and ensured connectedness. Only the connected road network was kept for analysis, removing isolated and disconnected pieces. For each road category, travel speed values were assigned speeds of 60 km/h, 40 km/h, and 20 km/h, for primary, secondary, and tertiary roads respectively. The transportation time for each section was calculated using the Field Calculator tool in the Attribute Table by using the following formula:

$$t_i = (l_i / v_i) * 60 \quad (8)$$

t_i: Total travel time for section i (minutes)

l_i: The length of section i (km)

v_i: The average vehicle speed for section i (km/h)

60: Used to convert the transportation time from hours to minutes

These lower-than-statutory speed restrictions indicate realistic operating speeds in hilly terrain, where steep grades, significant curvature, and changeable road surface conditions limit automobile mobility. Furthermore, to estimate emergency response times more accurately without local traffic data, conservative speed assumptions were used. Service Area analysis was then undertaken utilizing 15, 30, 60, and 120-minute travel time thresholds to define fire station coverage in the study areas. In addition to the network-based analysis, road network, waterways, and waterbody polygon datasets were used for Euclidean distance analysis. This method measured fire suppression entity accessibility by calculating the straight-line distance from these characteristics to estimate spatial proximity. For Euclidean distance analysis of water bodies and rivers, datasets were pre-processed to reduce redundancy and overestimation. To avoid overlap and distance estimates, linear water features that matched waterway polylines were deleted.

3.4. Validation of Fire Risk Zone using MODIS historical data

The validation quantifies how many historical fire occurrence points (or area) fall inside each vulnerability zone to evaluate the model's reliability and prediction performance. Multilayer Historical Fire Occurrence/ Hotspot Data harmonized with vulnerability raster:

o NASA FIRMS

o MODIS Active Fire Data

o VIIRS 375m Active Fire Data Fire Radiative Power (FRP) information

4. Results & Discussion

4.1. Thematic Layer

The weight assigned to each parameter represents a multi-criteria decision-making approach used to evaluate various factors and determine their relative importance across multiple criteria (Saaty et al., 2008; Mardani et al., 2015). In this study, the weighted values for each criterion were derived from the AHP worksheet, providing a systematic and objective basis for evaluating the contribution of each factor in the overall decision-making framework (Saaty et al., 2008; Mardani et al., 2015) (Table 6). Below figures (Figure 3,4,5,6) represent all the layers.

Table 6 Final weights of different features of thematic layer for assessment of forest fire zone

Description of factors	Weightage	Weightage %
Forest Type (FT)	20.7115	21
Normalized Difference Moisture Index (NDMI)	18.6812	19
Fire Occurrence Intensity (FPI)	14.3556	14
Normalized Difference Vegetation Index (NDVI)	12.1692	12
Aspect (A)	6.8343	7
Slope (S)	8.0121	8
Elevation (6)	6.3216	6
Standardized Precipitation Index (SPI)	3.3117	3
Land Surface Temperature (LST)	3.2742	3
Topographic Wetness Index (TWI)	2.5247	3
Windspeed (WS)	1.5883	2
Distance from Agriculture (DA)	1.2170	1
Distance from Settlement	0.9985	1

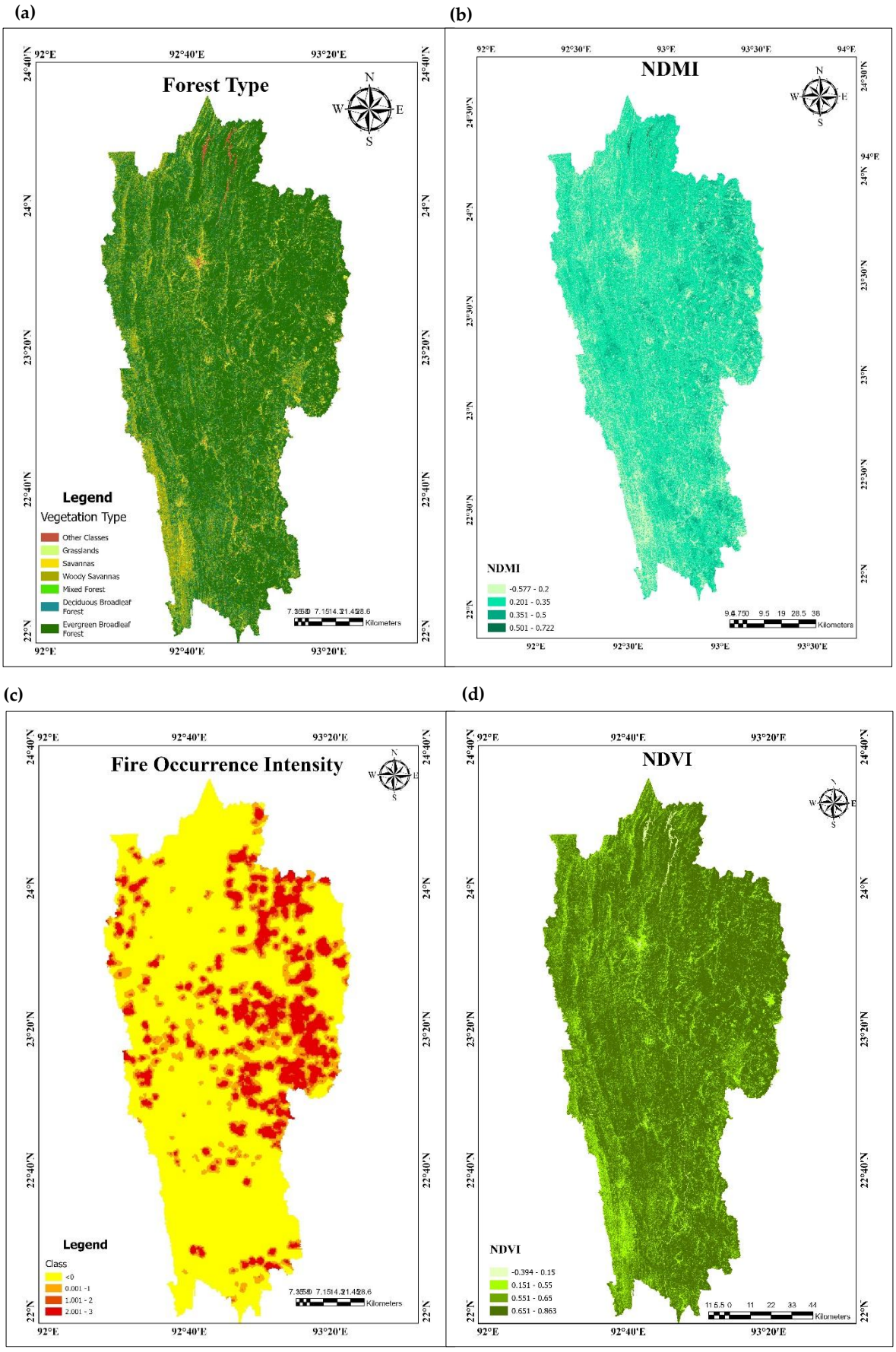


Figure 1 (a) Forest Type, (b) NDMI, (c) Fire Occurrence Intensity, and (d) NDVI map of Mizoram

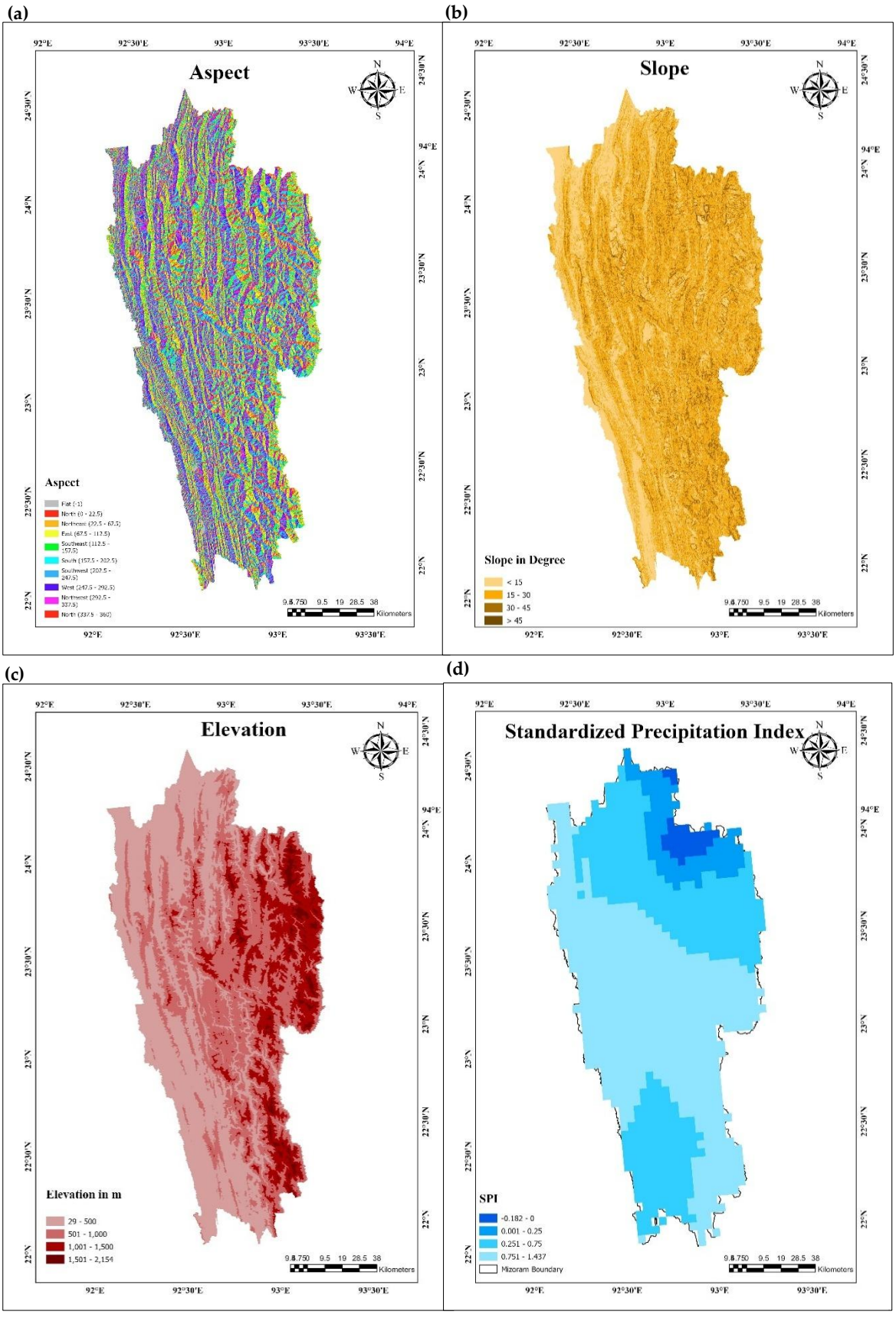


Figure 2 (a) Aspect, (b) Slope, (c) Elevation, and (d) SPI map of Mizoram

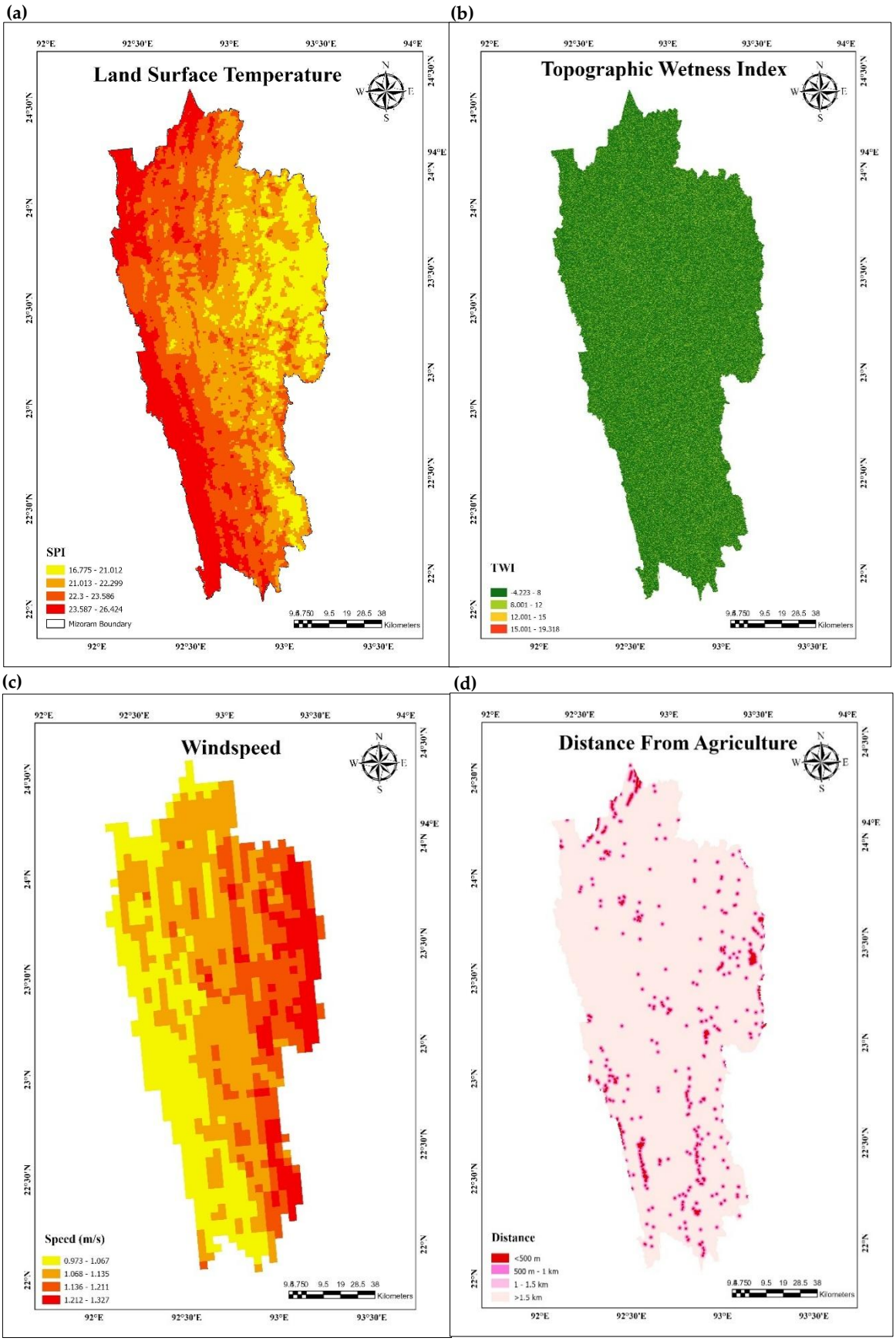


Figure 3 (a) LST, (b) TWI, (c) Windspeed, and (d) Distance from Agriculture map of Mizoram

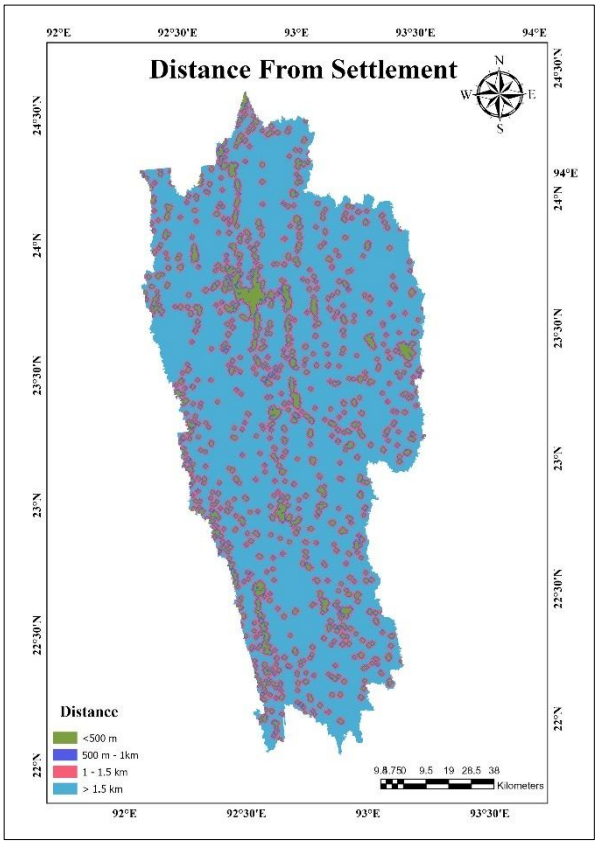


Figure 4 Distance from Settlement map of Mizoram

The below table (Table 7) is an assessment of the consistency of the pairwise comparisons performed for multi-criteria decision-making (AHP Matrix shown in Appendix). Nine criteria were evaluated, resulting in a maximum eigenvalue (λmax) of 14.15 for the matrix. The Consistency Index (CI) was determined to be 0.10963, indicating a satisfactory level of coherence in the evaluations. The Consistency Ratio (CR), which evaluates the acceptability of the Consistency Index (CI) against a standard threshold, was 0.06, signifying that the comparisons are predominantly consistent.

Table 7 Consistency Index (CI) and Ratio (CR) Calculation

λ_{max}	n	n - 1	λ_{max} - n	CI	RI	CR
14.15	13	12	1.15	0.0963	1.56	0.06

4.2. Evaluation of Forest Fire Risk Zones

Further, Fire risk zones were categorized into four classifications: very high, high, moderate, and low risk zones. The district-specific fire vulnerability zone map is illustrated in the Figure 7. Table 8 indicates that around 58% of the overall region is classified as very susceptible. 0.5% and 36% are into the categories of extremely high and moderate vulnerability zones, respectively. Consequently, over 90% of the total territory is susceptible to acute fire. The necessity of active, stratified, and spatially targeted fire management strategies is underscored by the considerable area that is subject to very high, high, and moderate fire vulnerability.

Table 8 Fire Vulnerability Risk Zonation

Forest fire Classes	Area in Km²	Area in Percentage %
Low	4.60	0.02
Moderate	8013	36
High	12732	58
Very High	120	0.5

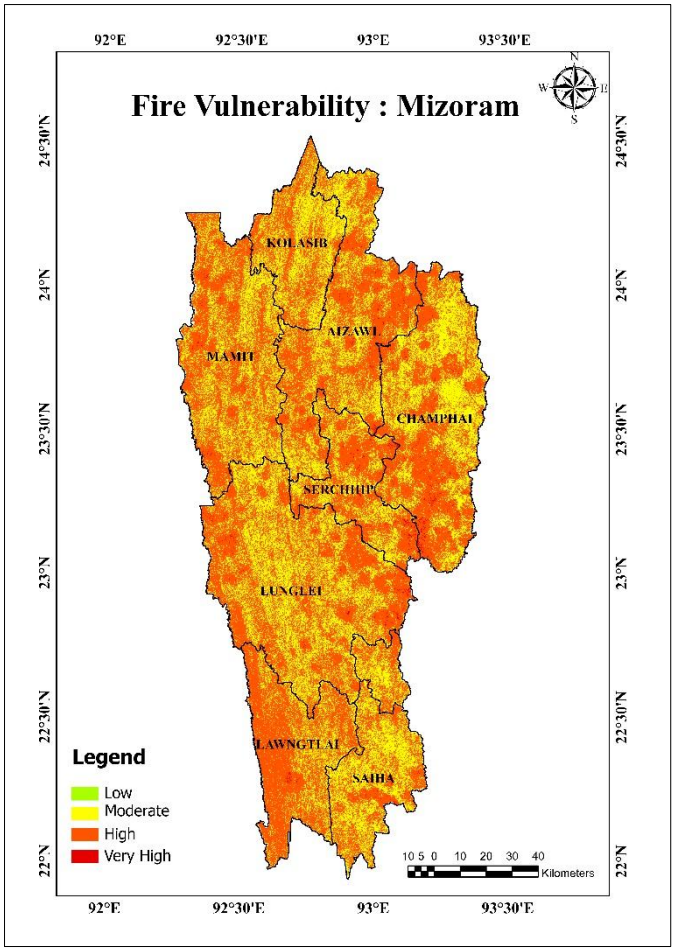


Figure 5 District-wise Forest Fire Vulnerability Zonation of Mizoram from low to very high

4.3. Proximity & Service-Area Analysis

Network analysis showed that only 9% of the areas were highly accessible within the critical response time 15 minutes, while 11% were nearly high accessible within the critical response time of 30 minutes under the current configuration of response teams. Inadequate road connectivity and challenging terrain hinder accessibility, exposing deficiencies in emergency coverage and necessitating enhanced station placement and road infrastructure. The findings underscore the necessity for better spatial positioning of response stations, enhanced road connection, and intentional redistribution or augmentation of firefighting personnel to minimize travel time and improve response efficiency along ideal network routes.

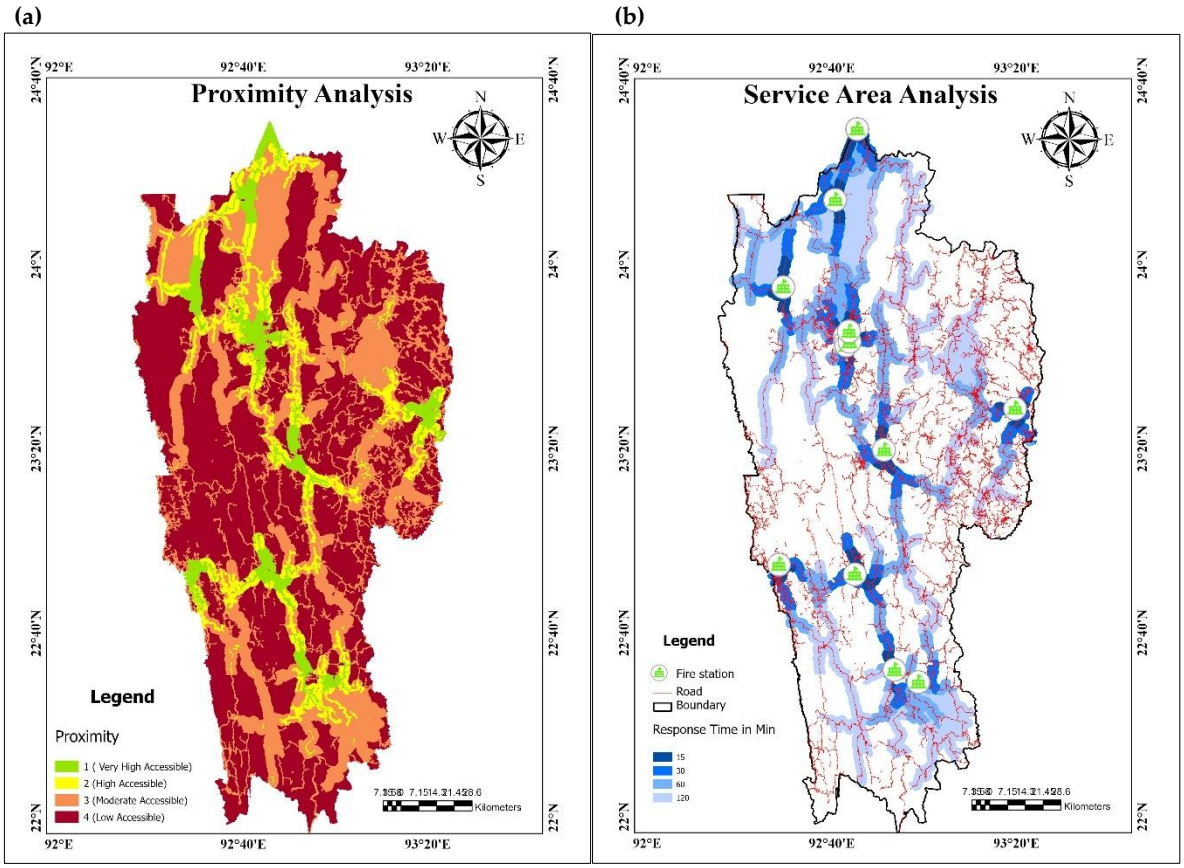


Figure 6 (a) Proximity Analysis, (b) Service Area Analysis

4.4 Resource Allocation

Resource allocation for forest fire suppression units pertains to the methodical and geographically informed distribution of firefighting assets to guarantee prompt response and efficient containment of fire occurrences, especially in high-risk zones. A resource allocation map was created by overlaying the forest fire vulnerability zones, focusing on areas designated as high and very high susceptibility, based on proximity and accessibility evaluations. The map indicates the required allocation of district-wise firefighting resources for effective fire suppression in these critical zones. Based on this comprehensive spatial analysis, strategic placement of new fire stations or sub-stations, extra firefighting teams, mobile suppression units, and road infrastructure upgrades were recommended. The allocation framework focused although presence of existing fire suppression unit, suggestive resource allocation required in the east of Aizawl, south of Champhai, and southwest of Lawngtlai due to highly vulnerable zones. Figure 9 shows the requirement of district-wise suggestive sites for fire suppression units.

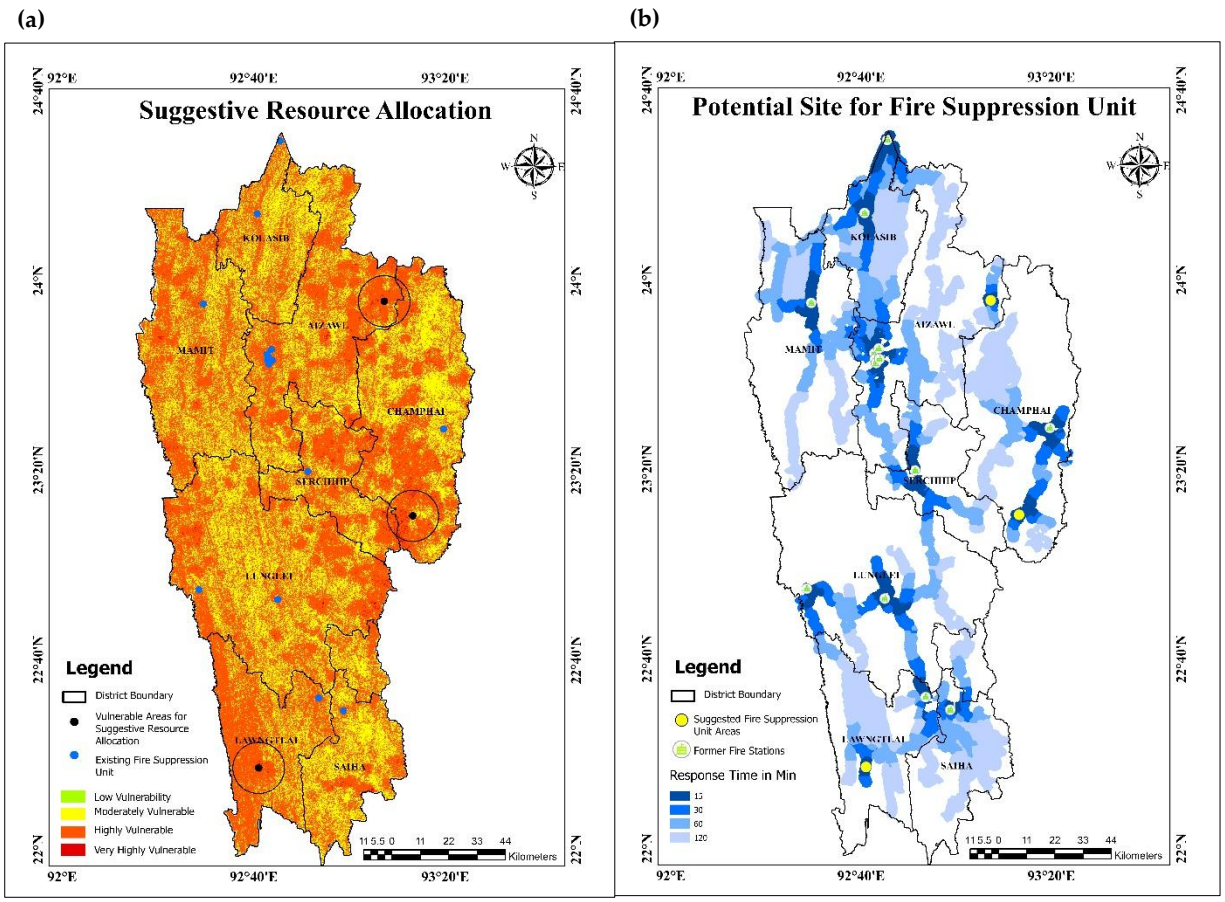


Figure 9 District-wise (a) Suggestive Resource Allocation based on vulnerable zones, (b) Potential Site for Fire Suppression Unit based on response time.

4.5. Validation of Forest Fire Risk Zone

The validation verifies that the AHP-based Forest Fire Vulnerability Model exhibits significant spatial concordance with historical fire occurrence locations and hotspot datasets. Historical fire occurrence data (fire counts) were employed for validation, demonstrates 64% of historical fire occurrence points fall within high and very high vulnerability zones, which together cover 62% of the study area**,** indicating reasonable model performance, which also reveals distinct spatial variability and fire density across vulnerability categories, normalized as fire point density (events per km²). High vulnerability zones exhibit the greatest fire incidence (60,065 events) and occupy a significant spatial extent, underscoring their dominant contribution to overall fire activity. Moderately vulnerable areas also demonstrate substantial fire occurrence (34,938 events), indicating persistent and recurrent burning patterns within these landscapes. Density-based assessment further indicates that high and very high vulnerability classes register approximately 5 fire detections per km², whereas low vulnerability zones exhibit a markedly lower density of < 2 detections per km², reflecting comparatively reduced fire susceptibility and activity. This spatial correspondence suggests that the developed vulnerability framework adequately represents the combined influence of biophysical characteristics and accessibility conditions that govern fire susceptibility, thereby

supporting its reliability for identifying fire prone landscapes. Table 9 and Figure 10 shows fire point statistics for Mizoram.

Table 9 Fire Occurrence Points based on Vulnerability Class

Class	Fire occurrences	Fire Points (%)	Area (km²)	Area (%)	Fire Point/km²
Low Vulnerable	12	0.01	4.60	0.02	~2
Moderately Vulnerable	34938	37	8013	36	~4
Highly Vulnerable	60065	63	12732	58	~5
Very Highly Vulnerable	501	0.55	112	0.5	~5

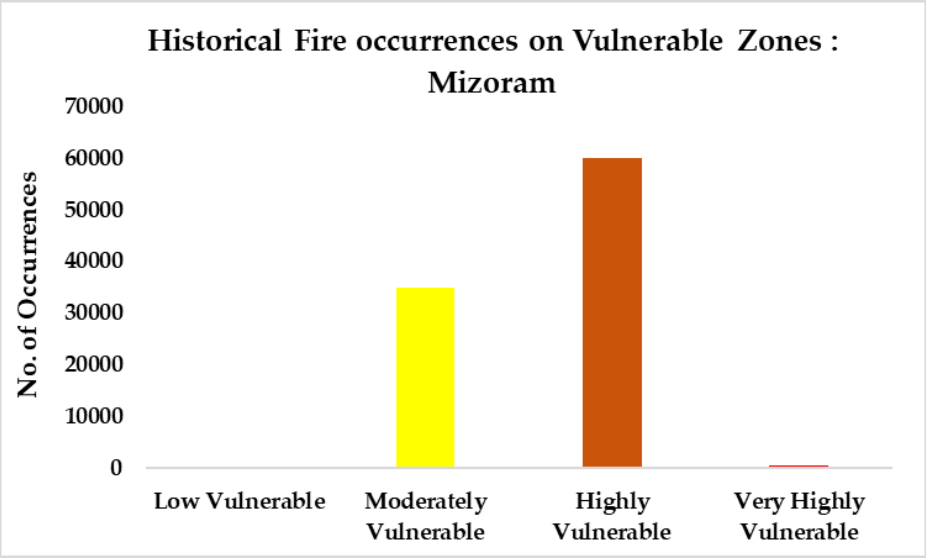


Figure 10 No. of Fire Occurrences on Vulnerable Zone

4.6. Limitations

The AHP weighting in this study is derived from validated literature and research conducted by regional government agencies, including the North-eastern Space Applications Centre (NESAC, 2014) and similar regions. The arrangement of parameters adhered to a uniform framework aligned with prior studies to guarantee methodological consistency and aid in the development of the pairwise comparison matrix. The reliability of outputs is influenced by the quality of input datasets; certain climatic layers, such as SPI and LST, were available at coarser resolutions (like, ~1 km to several kilometers). In integrated geospatial analyses, particularly those combining climatic, environmental, and high-resolution land surface data (like, Sentinel at 10 m), resampling is a necessary and standard pre-processing step to ensure spatial compatibility across datasets. Resampling was conducted to support pixel-level alignment and overlay analysis within a coherent spatial framework, allowing integration with higher-resolution layers utilized in the study. Appropriate resampling techniques, such as bilinear or cubic interpolation, were utilized to maintain spatial gradients and reduce distortion.

In the accessibility analysis, the OSM road network required substantial cleaning, leading to the removal of several disconnected or misclassified segments, particularly in remote and mountainous regions. This reduced network connectivity likely affected service area

delineation and may have underestimated accessibility in certain locations. The service area analysis was based on assumed travel speeds ranging from 20-75 km/h depending on road hierarchy. Although these values are lower than statutory speed limits, they were deliberately adopted to represent realistic operating conditions in Mizoram's hilly terrain, where vehicular movement is constrained by steep gradients, sharp curvature, and variable road surface conditions. In the absence of detailed local traffic and road condition data, these conservative assumptions were used to estimate emergency response times. Service areas were delineated using travel time thresholds of 15, 30, 60, and 120 minutes; however, actual response times may vary significantly due to seasonal factors (e.g., monsoon-related disruptions), terrain constraints, and road quality. Consequently, accessibility estimates may be subject to both over- and under-estimation in real-world scenarios. Despite these limitations, the framework provides a spatially explicit basis for relative prioritization and strategic planning**,** particularly in identifying high-risk zones and guiding the placement of fire suppression resources in data-scarce, mountainous landscapes.

5. Conclusion

This study explores the application of GIS and AHP method to assess fire risk in Mizoram, India. In this study, 13 parameters used for assessing fire risk reveals risk zone categorized into four zones as very high, high, moderate, and low risk. High and very high fire risk occupies 59% followed by moderate risk 36% of the study area. Proximity and service area-based network study indicate that only 9% of the places are highly accessible within the critical response time of 15 minutes, while 11% are virtually highly accessible within the critical response time of 30 minutes under the existing configuration of response teams. Potential locations for the establishment of firefighting units were suggested in Aizawl, Champhai, and Lawngtlai districts, owing to their high vulnerability and insufficient fire suppression resources. Additionally, the methodology employed in this study is applicable to other areas of Northeast India where forest fires pose significant challenges.

6. Data Availability

The datasets used in this study were from publicly available repositories. The processed datasets generated and analysed in this investigation are available from the corresponding author upon reasonable request.

7. Acknowledgements

The authors extend their sincere appreciation to the Director General of The Energy and Resources Institute, TERI, New Delhi, for providing institutional support, research facilities and a conducive environment that enabled the successful completion of this study. This research was conducted as part of an ICIMOD-supported project on forest fire management and air quality improvement in the Hindu Kush Himalaya region. The authors gratefully acknowledge the International Centre for Integrated Mountain Development, ICIMOD, as the

funding and coordinating agency for the project, and for facilitating collaboration and stakeholder engagement.

8. Declarations

Ethics declaration: Not applicable. This study used publicly available geospatial, remote sensing and secondary datasets and did not involve human participants, human data, animals or clinical trial procedures.

Consent to participate declaration: Not applicable.

Consent to publish declaration: Not applicable.

Clinical trial registration: Not applicable.

Competing interests: The authors declare that they have no competing interests.

Funding: This study was developed as part of an ICIMOD-supported project on forest fire management and air quality improvement in the Hindu Kush Himalaya region. No separate or dedicated funding was received specifically for the preparation of this manuscript.

Author contributions: M.M. carried out data compilation, preprocessing, GIS analysis, AHP-based vulnerability modelling, network and service-area analysis, preparation of maps and figures, and initial drafting of the manuscript. S.G. conceptualized the study, designed the methodological framework, supervised the analysis, interpreted the results, and led manuscript writing, review and editing. J.V.S. provided overall guidance, technical inputs, supervision and critical review of the manuscript. All authors reviewed and approved the final version of the manuscript.

Appendix

Table 1 Pairwise comparison matrix of the thematic layers

	FT	NDMI	FPI	NDVI	A	S	E	SPI	LST	TWI	WS	DA	DS
FT	1	2	2	3	4	4	5	6	6	7	9	9	9
NDMI	1/2	1	2	3	4	4	5	7	7	7	9	9	9
FPI	1/2	1/2	1	2	3	3	4	5	6	7	9	9	9
NDVI	1/3	1/3	1/2	1	3	3	4	5	5	6	9	9	9
A	1/4	1/4	1/3	1/3	1	1	2	3	3	3	5	7	9
S	1/4	1/4	1/3	1/3	1	1	2	3	5	5	7	9	9
E	1/5	1/5	1/4	1/4	1/2	1/2	1	2	3	5	7	9	9
SPI	1/6	1/7	1/5	1/5	1/3	1/3	1/2	1	1	2	3	4	5
LST	1/6	1/7	1/6	1/5	1/3	1/5	1/3	1	1	1	3	5	7
TWI	1/7	1/7	1/7	1/6	1/3	1/5	1/5	1/2	1	1	2	3	5
WS	1/9	1/9	1/9	1/9	1/5	1/7	1/7	1/3	1/3	1/2	1	2	3
DA	1/9	1/9	1/9	1/9	1/7	1/9	1/9	1/4	1/5	1/3	1/2	1	2
DS	1/9	1/9	1/9	1/9	1/9	1/9	1/9	1/5	1/7	1/5	1/3	1/2	1
SUM	**3.84**	**5.30**	**7.26**	**10.82**	**17.95**	**17.60**	**24.40**	**34.28**	**38.68**	**45.03**	**64.83**	**76.5**	**86**

Table 2 Normalized pairwise comparison matrix.

	FT	NDMI	FPI	NDVI	A	S	E	SPI	LST	TWI	WS	DA	DS	Total Wt	CW	CW %	CW %
FT	0.26	0.38	0.28	0.28	0.22	0.23	0.20	0.18	0.16	0.16	0.14	0.12	0.10	2.69	0.21	20.71	21
NDMI	0.13	0.19	0.28	0.28	0.22	0.23	0.20	0.20	0.18	0.16	0.14	0.12	0.10	2.43	0.19	18.68	19
FPI	0.13	0.09	0.14	0.18	0.17	0.17	0.16	0.15	0.16	0.16	0.14	0.12	0.10	1.87	0.14	14.36	14
NDVI	0.09	0.06	0.07	0.09	0.17	0.17	0.16	0.15	0.13	0.13	0.14	0.12	0.10	1.58	0.12	12.17	12
A	0.07	0.05	0.05	0.03	0.06	0.06	0.08	0.09	0.08	0.07	0.08	0.09	0.10	0.89	0.07	6.83	7
S	0.07	0.05	0.05	0.03	0.06	0.06	0.08	0.09	0.13	0.11	0.11	0.12	0.10	1.04	0.08	8.01	8
E	0.05	0.04	0.03	0.02	0.03	0.03	0.04	0.06	0.08	0.11	0.11	0.12	0.10	0.82	0.06	6.32	6
SPI	0.04	0.03	0.03	0.02	0.02	0.02	0.02	0.03	0.03	0.04	0.05	0.05	0.06	0.43	0.03	3.31	3
LST	0.04	0.03	0.02	0.02	0.02	0.01	0.01	0.03	0.03	0.02	0.05	0.07	0.08	0.43	0.03	3.27	3
TWI	0.04	0.03	0.02	0.02	0.02	0.01	0.01	0.01	0.03	0.02	0.03	0.04	0.06	0.33	0.03	2.52	3
WS	0.03	0.02	0.02	0.01	0.01	0.01	0.01	0.01	0.01	0.01	0.02	0.03	0.03	0.21	0.02	1.59	2
DA	0.03	0.02	0.02	0.01	0.01	0.01	0.00	0.01	0.01	0.01	0.01	0.01	0.02	0.16	0.01	1.22	1
DS	0.03	0.02	0.02	0.01	0.01	0.01	0.00	0.01	0.00	0.00	0.01	0.01	0.01	0.13	0.01	1.00	1
														13		100	100

Table 3 Consistency Calculation

	FT	NDMI	FPI	NDVI	A	S	E	SPI	LST	TWI	WS	DA	DS	WSV	CW	WSV/CW
FT	0.21	0.37	0.29	0.37	0.27	0.32	0.32	0.20	0.20	0.18	0.14	0.11	0.09	3.06	0.21	14.76
NDMI	0.10	0.19	0.29	0.37	0.27	0.32	0.32	0.23	0.23	0.18	0.14	0.11	0.09	2.83	0.19	15.16
FPI	0.10	0.09	0.14	0.24	0.21	0.24	0.25	0.17	0.20	0.18	0.14	0.11	0.09	2.16	0.14	15.07
NDVI	0.07	0.06	0.07	0.12	0.21	0.24	0.25	0.17	0.16	0.15	0.14	0.11	0.09	1.85	0.12	15.17
A	0.05	0.05	0.05	0.04	0.07	0.08	0.13	0.10	0.10	0.08	0.08	0.09	0.09	0.99	0.07	14.48
S	0.05	0.05	0.05	0.04	0.07	0.08	0.13	0.10	0.16	0.13	0.11	0.11	0.09	1.16	0.08	14.50
E	0.04	0.04	0.04	0.03	0.03	0.04	0.06	0.07	0.10	0.13	0.11	0.11	0.09	0.88	0.06	13.98
SPI	0.03	0.03	0.03	0.02	0.02	0.03	0.03	0.03	0.03	0.05	0.05	0.05	0.05	0.46	0.03	13.83
LST	0.03	0.03	0.02	0.02	0.02	0.02	0.02	0.03	0.03	0.03	0.05	0.06	0.07	0.44	0.03	13.40
TWI	0.03	0.03	0.02	0.02	0.02	0.02	0.01	0.02	0.03	0.03	0.03	0.04	0.05	0.34	0.03	13.52
WS	0.02	0.02	0.02	0.01	0.01	0.01	0.01	0.01	0.01	0.01	0.02	0.02	0.03	0.21	0.02	13.36
DA	0.02	0.02	0.02	0.01	0.01	0.01	0.01	0.01	0.01	0.01	0.01	0.01	0.02	0.16	0.01	13.33
DS	0.02	0.02	0.02	0.01	0.01	0.01	0.01	0.01	0.00	0.01	0.01	0.01	0.01	0.13	0.01	13.47
															λ max	14.15596

References

Agee, J. K. (1993). Fire ecology of Pacific Northwest forests. Island Press. https://islandpress.org/books/fire-ecology-pacific-northwest-forests

Bera B, Shit PK, Sengupta N, Saha S, Bhattacharjee S (2022) Forest fire susceptibility prediction using machine learning models with resampling algorithms, northern part of Eastern Ghat Mountain range (India). Geocarto Int 37(26):11756–11781. https://doi.org/10.1080/10106049.2022.2060323

Bergonse, R., Oliveira, S., Gonçalves, A., Nunes, S., DaCamara, C., & Zêzere, J. L. (2021). Predicting burnt areas during the summer season in Portugal by combining wildfire susceptibility and spring meteorological conditions. Geomatics, Natural Hazards and Risk, 12(1), 1039–1057. https://doi.org/10.1080/19475705.2021.1909664

Beven, K. J., & Kirkby, M. J. (1979). A physically based, variable contributing area model of basin hydrology. Hydrological Sciences Bulletin, 24(1), 43–69. https://doi.org/10.1080/02626667909491834

Brown, S. (1997). Present and potential roles of forests in the global climate change debate. FAO. https://www.fao.org/4/w0312e/w0312e03.htm

Chaudhary SK, Pandey AC, Parida BR (2022) Forest fire characterization using Landsat-8 satellite data in Dalma Wildlife Sanctuary. Remote Sens Earth Syst Sci 5(4):230–245. https://doi.org/10.1007/s41976-022-00076-3

Cooke, W. H., Mostovoy, G. V., Anantharaj, V. G., & Jolly, W. M. (2012). Wildfire potential mapping over the state of Mississippi: A land surface modeling approach. GIScience & Remote Sensing.

Cruz, M. G., Alexander, M. E., & Wakimoto, R. H. (2003). Modelling the wind field produced by a line fire. International Journal of Wildland Fire, 12(4), 421–430.

Eckdahl, J. A., Kristensen, J. A., & Metcalfe, D. B. (2022). Climatic variation drives loss and restructuring of carbon and nitrogen in boreal forest wildfire. Biogeosciences, 19, 2487–2506. https://doi.org/10.5194/bg-19-2487-2022

Elia, M., D'Este, M., Ascoli, D., Giannico, V., Spano, G., Ganga, A., Colangelo, G., Lafortezza, R., & Sanesi, G. (2020). Estimating the probability of wildfire occurrence in Mediterranean landscapes using artificial neural networks. Environmental Impact Assessment Review, 85, 106474. https://doi.org/10.1016/j.eiar.2020.106474

Forest Survey of India**.** (2023). India state of forest report 2023 (ISFR 2023). Ministry of Environment, Forest and Climate Change, Government of India. https://fsi.nic.in/uploads/isfr2023/isfr_book_eng-vol-1_2023.pdf

Ghorbanzadeh, O., Valizadeh Kamran, K., Blaschke, T., Aryal, J., Naboureh, A., Einali, J., & Bian, J. (2019). Spatial prediction of wildfire susceptibility using field survey GPS data and machine learning https://doi.org/10.3390/fire2030043

Gill, A. M. (1975). Fire and the Australian flora: A review. Australian Forestry, 38(1), 4–25. https://doi.org/10.1080/00049158.1975.10675618

Goparaju, L., Pillutla, R. C. P., & Venkata, S. B. K. (2023). Assessment of forest fire emissions in Uttarakhand State, India, using Open Geospatial data and Google Earth Engine. Environmental Science and Pollution Research International, 30(45), 100873–100891. https://doi.org/10.1007/s11356-023-29311-0

Gupta A, Roy A, Chauhan P (2023) Space-based observation of early summer wildfire event and its environmental proxies during 2021 in Eastern Peninsular India. Arab J Geosci 16(7):433. https://doi.org/10.1007/s12517-023-11544-5

Hai, T., Sayed, B. T., Majdi, A., Zhou, J., Sagban, R., Band, S. S., & Mosavi, A. (2023). An integrated GIS-based multivariate adaptive regression splines–cat swarm optimization for improving the accuracy of wildfire susceptibility mapping. Geocarto International. https://doi.org/10.1080/10106049.2023.2167005

Jiang, P., Russell, M. B., Frelich, L., Babcock, C., & Smith, J. E. (2023). Wildfires correlate with reductions in aboveground tree carbon stocks and sequestration capacity on forest land in the Western United States. Science of the Total Environment, 893, 164832. https://doi.org/10.1016/j.scitotenv.2023.164832

Khan MA, Sharma P, Thangavel M, Ahmad M (2024) Spatio-temporal dynamics of wildfires in Hoshangabad Forest Division of Central India: a geospatial and statistical investigation. Lett Spat Resour Sci 17(1):28. https://doi.org/10.1007/s12076-024-00390-y

Kumar, A., Ray, T., Mohanasundari, T., Jatav, S. S., Chatterjee, U., Shekhar, S., Alam, E., & Islam, M. K. (2025). Forest fires and climate change in India: Impacts, adaptive strategies, and pathways for climate action (Sustainable Development Goal-13). Environmental Sciences Europe, 37**,** 147. https://doi.org/10.1186/s12302-025-01195-6

Kumar, S. (2024). Status of India's forests. In A. Srivastav (Ed.), Forest policies, laws, and governance in India: Conservation challenges in the face of climate change (pp. 207–232). Springer, Cham. https://doi.org/10.1007/978-981-97-3862-5_5

Li, F., Zhang, X., Kondragunta, S., & Csiszar, I. (2018). Comparison of fire radiative power estimates from VIIRS and MODIS observations. Journal of Geophysical Research: Atmospheres, 123(9), 4545–4563. https://doi.org/10.1029/2017JD027823

Lu, M. (2025, June 18). Infographic: How terrestrial carbon storage works. Visual Capitalist. https://www.visualcapitalist.com/infographic-how-terrestrial-carbon-storage-works/

MacCarthy, J., Richter, J., Tyukavina, S., Weisse, M., & Harris, N. (2025, July 21). The latest data confirms: Forest fires are getting worse. World Resources Institute. https://www.wri.org/insights/global-trends-forest-fires

Mardani, A., Jusoh, A., Zavadskas, E. K., Khalifah, Z., & Md Nor, K. (2015). Application of multiple-criteria decision-making techniques and approaches to evaluating of service quality: a systematic review of the literature. Journal of Business Economics and Management, 16(5), 1034–1068. https://doi.org/10.3846/16111699.2015.1095233

Mitchard, E. T. A. (2018). The tropical forest carbon cycle and climate change. Nature, 559, 527–534. https://www.nature.com/articles/s41586-018-0300-2

Mizoram State Climate Change Cell. (2023). District level climate change vulnerability assessment of Mizoram: Biophysical and socio-economic sectors [Report]. Mizoram Science, Technology & Innovation Council (MISTIC). https://mistic.mizoram.gov.in/wp-content/uploads/2023/04/Dist_Level_Climate_VA_of_Mizoram_Biophysical_Socioeconomic_Sectors_compressed.pdf

Moore, I. D., Gessler, P. E., Nielsen, G. A., & Peterson, G. A. (1993). Soil attribute prediction using terrain analysis. Soil Science Society of America Journal, 57(2), 443–452. https://doi.org/10.2136/sssaj1993.03615995005700020026x

Moritz, M. A., Batllori, E., Bradstock, R. A., Gill, A. M., Handmer, J., Hessburg, P. F., Leonard, J., McCaffrey, S., Odion, D. C., Schoennagel, T., & Syphard, A. D. (2014). Learning to coexist with wildfire. Nature, 515(7525), 58–66. https://doi.org/10.1038/nature13946

NESAC (North Eastern Space Applications Centre). (2014). Forest fire assessment and monitoring in Northeast India. Department of Space, Government of India. https://nesac.gov.in/assets/resources/2020/12/Forest-Fire-Assessment-in-NER.pdf

Nikolić, G., Vujović, F., Golijanin, J., Šiljeg, A., & Valjarević, A. (2023). Modelling of wildfire susceptibility in different climate zones in Montenegro using GIS-MCDA. Atmosphere, 14(6), 929. https://doi.org/10.3390/atmos14060929

Novković, I., Marković, G. B., Lukić, Đ., Dragićević, S., Milošević, M., Đurđić, S., Samardžić, I., Ležaić, T., & Tadić, M. (2021). GIS-based forest fire susceptibility zonation with IoT sensor network support, case study—Nature Park Golija, Serbia. Sensors, 21(19), 6520. https://doi.org/10.3390/s21196520

Olaniya, M., Bora, P. K., Das, S., & Chanu, P. H. (2020). Soil erodibility indices under different land uses in Ri-Bhoi district of Meghalaya (India). Scientific Reports, 10, Article 14986. https://doi.org/10.1038/s41598-020-72070-y

Pourtaghi, Z. S., Pourghasemi, H. R., & Rossi, M. (2015). Forest fire susceptibility mapping in the Minudasht forests, Golestan province, Iran. Environmental Earth Sciences, 73(4), 1515–1533. https://doi.org/10.1007/s12665-014 3502-4

Pyne, S. J. (1997). The current fire scene. In Fire in America: A cultural history of wildland and rural fire (pp. 1–25). University of Washington Press.

Rahmati, O., Nazari Samani, A., Mahdavi, M., Pourghasemi, H. R., & Zeinivand, H. (2015). Groundwater potential mapping at Kurdistan region of Iran using analytic hierarchy process and GIS. Arabian Journal of Geosciences, 8(9), 7059–7071. https://doi.org/10.1007/s12517-014-1668-4

Reid, C. E., Brauer, M., Johnston, F. H., Jerrett, M., Balmes, J. R., & Elliott, C. T. (2016). Critical review of health impacts of wildfire smoke exposure. Environmental Health Perspectives, 124(9), 1334–1343. https://doi.org/10.1289/ehp.1409277

Revich BA (2024) Climate change and forest fires as health risk factors (Analytical review). Health Risk Anal. https://doi.org/10.21668/health.risk/2024.3.14

Rihan, W., Zhao, J., Zhang, H., Guo, X., Ying, H., Deng, G., & Li, H. (2019). Wildfires on the Mongolian Plateau: Identifying drivers and spatial distributions to predict wildfire probability. Remote Sensing, 11(20), 2361. https://doi.org/10.3390/rs11202361

Rihan, W., Zhao, J., Zhang, H., Guo, X., Ying, H., Deng, G., & Li, H. (2019). Wildfires on the Mongolian Plateau: Identifying drivers and spatial distributions to predict wildfire probability. https://doi.org/10.3390/rs11202361

Riley, K. L., Mockrin, M. H., & Loehman, R. A. (2020). Wildland fire at the wildland–urban interface in the USA: A spatial analysis of homes and fire danger. Landscape and Urban Planning, 197, 103759.

Saaty TL (1980) The analytic hierarchy process: planning, priority setting and resource allocation. McGraw-Hill, New York, pp 1–287

Saaty, T. L. (2008). Decision making with the analytic hierarchy process. International Journal of Services Sciences, 1(1), 83–98. https://doi.org/10.1504/IJSSCI.2008.017590

Saxena A, Güneralp B (2022) Understanding the dynamics between forest landscapes and rural livelihoods: a case study from Central India. Springer, Cham. https://doi.org/10.1007/978-3-030-88555-7_14

Sewak, R., Vashisth, M., & Gupta, L. (2021). Forest fires in India: A review. Journal of University of Shanghai for Science and Technology, 23(7), 247–259. https://doi.org/10.51201/JUSST/21/07129

Taylor, S. W., Woolford, D. G., & Ghiloufi, W. (2006). A review of the prescribed burning program in boreal forests of Ontario. Forest Ecology and Management, 234(1–3), 218–228.

Tripathi, S. K., Upadhyay, K. K., & Singh, N. S. (2020). Forest fire in Mizoram: An overview. Mizoram University. https://www.researchgate.net/publication/350723628

Walker, X. J., Mack, M. C., Black, B. A., Barger, N. N., Rupp, T. S., & Hu, F. S. (2025). Increasing wildfire frequency decreases carbon storage and leads to regeneration failure in Alaskan boreal forests. Fire Ecology, 21, Article 57. https://doi.org/10.1186/s42408-025-00390-3

Williams, N. G., Lucash, M. S., Ouellette, M. R., Brussel, T., Gustafson, E. J., Weiss, S. A., … & Shvidenko, A. Z. (2023). Simulating dynamic fire regime and vegetation change in a warming Siberia. Fire Ecology, 19(1), 33.https://fireecology.springeropen.com/articles/10.1186/s42408-023-00188-1

Wu, B., Song, Z., Wu, Q., Wu, J., & Yu, B. (2023). A vegetation nighttime condition index derived from the triangular feature space between nighttime light intensity and vegetation index. IEEE Transactions on Geoscience and Remote Sensing, 61, 1–15. https://doi.org/10.1109/TGRS.2023.3305457

Yang, X., Jin, X., & Zhou, Y. (2021). Wildfire risk assessment and zoning by integrating Maxent and GIS in Hunan Province, China. Forests, 12(10), 1299. https://doi.org/10.3390/f12101299

Zhang, G., Wang, M., & Liu, K. (2021). Deep neural networks for global wildfire susceptibility modelling. Ecological https://doi.org/10.1016/j.ecolind.2021.107735

Zhang, G., Zhang, L., Li, X., Feng, X., Wang, Y., Guo, J., Liu, H., Chen, Z., & Wei, X. (2025a). Spatiotemporal evolution characteristics and driving mechanisms of wildfires in China under the context of climate change and human activities. Ecological Indicators, 176, 113694. https://doi.org/10.1016/j.ecolind.2025.113694

Zhang, Y., Lim, H. S., Hu, C., & Zhang, R. (2024). Spatiotemporal dynamics of forest fires in the context of climate change: A review. Environmental Science and Pollution Research International. https://pubmed.ncbi.nlm.nih.gov/38662294/

Zhao, B., Zhuang, Q., Shurpali, N., Köster, K., Berninger, F., & Pumpanen, J. (2021). North American boreal forests are a large carbon source due to wildfires from 1986 to 2016. Scientific Reports, 11, Article 7723. https://doi.org/10.1038/s41598-021-87343-3